LANGMUIR

pubs.acs.org/Langmuir Article

Photo-Detachable Self-Cleaning Surfaces Inspired by Gecko Toepads

Xiaohang Luo, $^{\nabla}$ Xiaoxiao Dong, $^{\nabla}$ Yanguang Hou, Lifu Zhang, Penghao Zhang, Jiaye Cai, Ming Zhao, Melvin A. Ramos, Travis Shihao Hu, Hong Zhao, and Quan Xu*



Cite This: Langmuir 2021, 37, 8410-8416



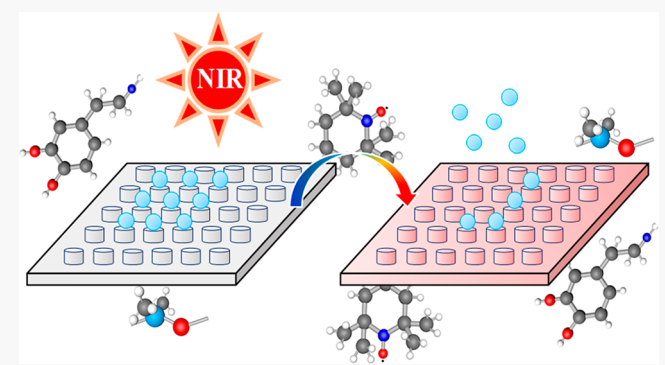
ACCESS

Metrics & More



SI Supporting Information

ABSTRACT: Strong, reversible, and self-cleaning adhesion in the toe pads of geckos allow the lizards to climb on a variety of vertical and inverted surfaces, regardless of the surface conditions, whether hydrophobic or hydrophilic, smooth or tough, wet or dry, clean or dirty. Development of synthetic gecko-inspired surfaces has drawn a great attention over the past two decades. Despite many external-stimuli responsive mechanisms (i.e., thermal, electrical, magnetic) have been successfully demonstrated, smart adhesives controlled by light signals still substantially lag behind. Here, in this report, we integrate tetramethylpiperidinyloxyl (TEMPO)-doped polydopamine (PDA), namely, TDPDA, with PDMS micropillars using a template-assisted casting method, to achieve both improved adhesion and self-cleaning performances. To the best of our



knowledge, this is the first report on PDA being used as a doping nanoparticle in bioinspired adhesive surfaces to achieve highly efficient self-cleaning controllable by light signals. Notably, the adhesion of the 5% TDPDA-PDMS sample is ~688.75% higher than that of the pure PDMS at the individual pillar level, which helps to explain the highly efficient self-cleaning mechanism. The sample surfaces (named TDPDA-PDMS) can efficiently absorb 808 nm wavelength of light and heat up from 25 °C to 80.9 °C in 3 min with NIR irradiation. The temperature rise causes significant reduction of adhesion, which results in outstanding self-cleaning rate of up to 55.8% within five steps. The exploration of the photoenabled switching mechanism with outstanding sensitivity may bring the biomimetic smart surfaces into a new dimension, rendering varied applications, e.g., in miniaturized climbing robot, artificial intelligence programmable manipulation/assembly/filtration, active self-cleaning solar panels, including high output sensors and devices in many engineering and biomedical frontiers.

INTRODUCTION

Nature does nothing in vain. Over 4 billion years, organisms have evolved countless intriguing structures with multifunctionalities adaptive to the complex and dynamic environment. For example, cactus are able to effetely collecting water from moisture in the air to resist drought; 2,3 the shellfish rely on a hard and tough exoskeleton to resist external damage; 4,3 and tree frogs,⁶ geckos,⁷⁻¹³ and mussels^{14,15} have strong and versatile adhesion capabilities to secure and maneuver on various surfaces. Among them, the gecko lizards have attracted a great deal of attention, because of their unique reversible adhesion and self-cleaning properties. The toe pad of a gecko has millions of small fibrils named setae and each seta can further branch into hundreds of smaller branches, known as spatulae. It is evident solely relying on van der Waals forces, a single toe of gecko can support 10 times of its body weight. 7,8 By controlling the angles between the setal stalks and contact surfaces, geckos can swiftly switch from attachments to detachments. In addition, geckos can walk on dusty surfaces without significant clogging or degradation, between the molting periods, showing astonishing self-cleaning ability and longevity. The dynamic and active self-cleaning mechanism have significant implications in the fields of manufacturing, electronics, robotics, etc. $^{16-18}$

Polymeric materials and carbon nanotubes are widely used to make bioinspired structures mimicking the foot hairs of the gecko. ^{19,20} Template-assisted micromolding/nanomolding of polymers offers great geometric controllability and selection of different intrinsic materials properties (in terms of strength, modulus, toughness, viscoelasticity, thermal plasticity, etc.), for example, using polydimethylsiloxane (PDMS), poly(methyl methacrylate) (PMMA), or polypropylene (PP). ^{21–24} On the other hand, carbon nanomaterials (CNTs obtained from

Received: February 27, 2021 Revised: June 15, 2021 Published: July 2, 2021





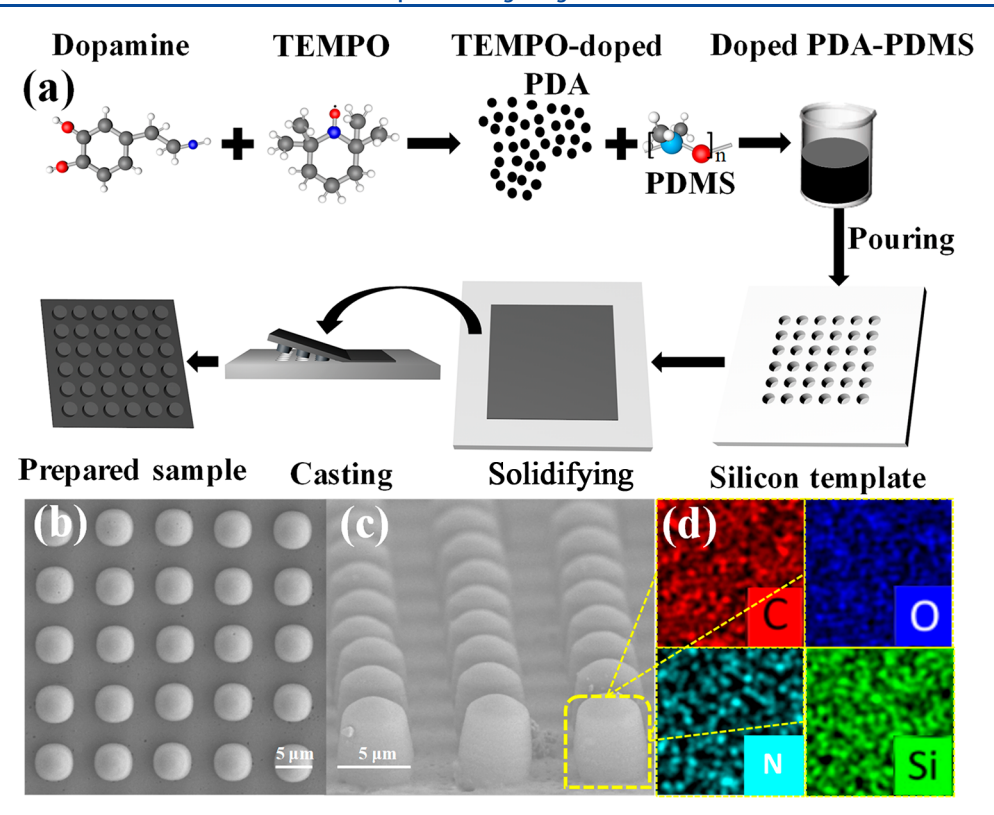


Figure 1. (a) Schematics of the process of preparing bioinspired adhesive samples; (b) top-view SEM images of the sample surfaces; (c) side-view SEM images of the sample surfaces; and (d) EDX mapping of the sample shows the elements of C, O, N, and Si from left to right.

chemical vapor deposition [CVD]) have excellent thermal, electrical, and mechanical properties, yet they are prone to fracture and damage from the substrates, and with often with random distributions and morphology. 25,26 There are also many other material candidates to choose to showcase the concept of "contact splitting" in scaling up strong adhesions. For instance, Murphy et al. were influenced by the idea of photolithography to produce a gecko biomimetic setae using SU-8 glue, and obtained a SU-8 biomimetic gecko adhesion surface with a hierarchical structure.²⁷ The fabrication of highaspect-ratio hierarchical arrays on flexible polycarbonate sheets by a sacrificial-layer-mediated nanoimprinting technique was also found and the dry-adhesive films comprising the hierarchical arrays showed a formidable shear adhesion.²⁴ However, when bioinspired surfaces realize the gecko adhesion function, the self-cleaning performance of the bionic gecko surfaces are seldom considered. At the same time, there are only a few researches on the biomimetic gecko surfaces can respond to the external environmental conditions to realize the dynamic control and manipulation of microparticles or dust

In order to be applied in more general situations and realize both the strong adhesion and self-cleaning characteristics seen in geckos, integrating functional nanoparticles could enable the biomimetic surfaces to be responsive to a variety types of external stimuli (i.e., thermal, electrical, magnetic), creating additionally levels of conformability and robustness. For example, doped Fe₃O₄ nanoparticles can be controlled by the external magnetic field, doped carbon quantum dots can enable the responsiveness to UV lamp irradiation. ^{28–30} However, there are still few studies on the smart adhesives controlled by NIR light signals, to the best of our knowledge. In addition, among a variety of nanoparticles, PDA has been

applied to realize many functions, such as antibacterial property,³¹ anticorrosion performance,³² and so on. In particular, polydopamine (PDA) has good photothermal properties, which can efficiently convert photon energy to heat energy.^{33–35} We hypothesize that taking advanced of PDA's photothermal properties will help to achieve highly efficient self-cleaning in gecko-inspired dry adhesives.

Herein, we report a noncontact surface control mechanism via light, which shows the active and direct control of adhesion with outstanding sensitivity, robustness, and durability. The samples were prepared as an innovative tetramethylpiperidinyloxyl-doped-polydopamine-polydimethylsiloxane (TDPDA-PDMS, also called a PDA-PDMS) composite. When exposed to light stimulus, the temperature increased from 25 °C to 80.9 °C in 3 min, and it can be repeated more than 30 times. PDMS-based biomimetic surfaces are created by adding the modified polydopamine (PDA), which has adhesion and photothermal properties. The surface demonstrates strong selfcleaning performance in the air. In addition, the strong photothermal properties from the addition of nanoparticles would reduce the adhesion of the surface when the surface is exposed under 808 nm near-infrared radiation (NIR). Those characteristics facilitate the separation process and enhance their self-cleaning performance. The outcomes have significant implications in the fields of smart adhesives, advanced manufacturing, counterspace exploration, renewable energy, and biomedical applications.

■ EXPERIMENTAL SECTION

Sample Preparation. TEMPO-doped PDA solution was prepared by a one-pot polymerization of TEMPO and dopamine in an aqueous solution at room temperature. The TEMPO (400 mg, 2.56 mmol) was fully dissolved in 80 mL of deionized water under

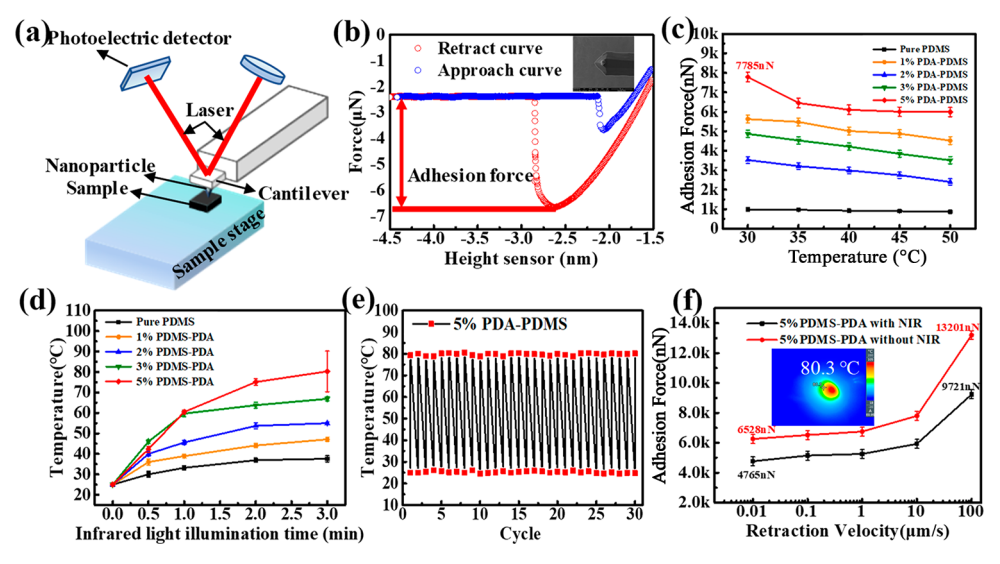


Figure 2. (a) Schematic of the setup of AFM pull-off test; The retraction velocity was kept as $3.08 \mu m/s$, the preloading force was kept as $1 \mu N$, and the contact time was kept as 2 s during the investigation of temperature effect on adhesion force. (b) Typical AFM force curve in the adhesion measurement. (c) Influence of temperature and mass content of PDA-PDMS samples on adhesion force. (d) Temperature elevation of five samples under NIR irradiation. (e) Temperature response curve of PDA-PDMS under 30 cycles of NIR irradiation. (f) Effect of NIR on the adhesion of samples of 5% PDA-PDMS under different retraction velocities.

magnetic stirring for 20 min. Dopamine hydrochloride (200 mg) was dissolved in 20 mL of deionized water and then quickly injected into above solutions. After stirring for 8–16 h, the TEMPO-doped PDA solution was prepared. PDMS was mixed with curing agent (Sylgard 184) at a ratio of 10:1. TEMPO-doped PDA solution (0, 1, 2, 3, and 5 wt %) was added into the PDMS mixture before curing. The mixture then was placed into a vacuum pump to degas. The template was placed into an environment with a temperature of 60 °C for 9 h.

Adhesion Tests of Bioinspired Surfaces. The atomic force microscopy (AFM) (Dimension Icon AFM, Bruker Co., Inc.) was adopted to study the adhesion performance of the bioinspired surfaces. To ensure nondestructive contact between AFM tip and sample surface, a nanosphere (nanosphere type: PS pellet with a diameter of $10~\mu m$) is attached to a tipless AFM probe (probe type: RTESPA-150, Bruker, Inc.). To fabricate the nanosphere modified probe, a PS was picked by a nanomanipulator and transferred to the desired location of a tipless AFM probe under scanning electron microscopy (SEM) (FEI Helios NanoLab, Cleveland, OH, USA), followed by a permanent gluing process. The temperature of the adhesive measured under light radiation was measured by the infrared imaging devices (Testo 865).

Self-Cleaning Capability Test. The LDP testing procedure of the bioinspired surfaces was used to simulate the self-cleaning process of the actual movement of gecko feet. At the initial stage, the bioinspired surfaces were fully covered with hydrophobic PS. The preload of the self-cleaning experiment was set up as ~2 N, and the velocity was controlled at ~1 cm/s. After each step of the LDP, the number of dropped pellets was counted to calculate the self-cleaning efficiency/rate of the bioinspired surfaces. The test conditions were as follows: 30 °C without NIR light, 50 °C without NIR light, and 30 °C with NIR light.

■ RESULTS AND DISCUSSION

Preparation and Characterization of Bioinspired Surface. In order to investigate the influences of TEMPOdoped PDA (TDPDA) on the self-cleaning performance, the addition of 0%, 1%, 2%, 3%, and 5% of TDPDA into the sample solutions were tested. The fabrication process of the bioinspired surfaces (TDPDA-PDMS surface) is illustrated in Figure 1a. Silicon templates cast the poured TDPDA solutions into the shape of micropillars. The micropillars

were obtained by peeling the cured samples from the templates. The SEM images show the morphology of the PDA–PDMS surfaces from different perspectives. From Figures 1b and 1c, the vertical micropillars showed an even distribution, with a diameter of \sim 5 μ m and a height of \sim 5 μ m. Energy-dispersive X-ray spectroscopy (EDX) was applied to map the distribution of different elements (C, O, N, and Si) in PDA–PDMS, as shown in Figure 1d. The N element only presented in the TDPDA solution. According to the EDX results, the TDPDA solution was successfully evenly dispersed in the PDMS system. The SEM image of TDPDA solutions is shown in Figure S1 in the Supporting Information.

The microstructures in pure PDMS samples significantly affected the surface adhesion, yet in the 5% doped TDPDA samples, the effects were not obvious. The contact angles difference between the pure PDMS samples with and without the microstructures was 27.8°, whereas the difference between the 5% TDPDA samples with and without the microstructures was only 4.4°. (See Figures S2a and S2b in the Supporting Information.) The angle difference indicated that the microstructures enhanced the hydrophobicity of bioinspired surfaces, while the doping of TDPDA solution decreased the enhancement of microstructures on the hydrophobic property of the surfaces. In addition, the contact angles of 5% doping PDA-PMS surfaces with and without microstructures were 27.6° and 28.6°, respectively, with ethyl alcohol droplets in the air (see Figure S2c in the Supporting Information).

Key Factors Influencing Adhesion Properties and NIR-Triggered Photothermal Effect on the Bioinspired Surfaces. The factors influencing the adhesive properties of the bioinspired surfaces, such as mass content of the TDPDA solution, temperature, contact time, preloading force, and retraction velocity, were systematically investigated. AFM) was adopted to test the adhesion force. The working principle of the AFM pull-off test is shown in Figure 2a, and a typical adhesion force curve is shown in Figure 2b. Herein, the samples with the mass fraction of 0%, 1%, 2%, 3%, and 5% of

TDPDA solution were fabricated and labeled as a, b, c, d, and e, respectively.

The increase of the mass percentage of TDPDA has a tendency to increase the adhesion force of the PDA-PDMS sample. The 5% PDA-PDMS sample showed the maximum initial adhesion force among all samples. Compared with the pure PDMS sample, the adhesion forces of the 5% PDA-PDMS samples increased by ~688.75% (see Figure 2c).

Temperature played a key role in the PDA-PDMS detaching process. All PDA-PDMS samples showed a significant temperature-dependent adhesion. The adhesion force of samples a, b, c, d, and e decreased by the amounts of 12.36%, 19.57%, 31.8%, 27.87%, and 23.10%, respectively, when the temperature was changed from 30 °C to 50 °C (Figure 2c). The 5% doping has excellent adhesion and its adhesion force varies with temperature. The results of the initial adhesion force and detaching characteristics indicated that the 5% PDA-PDMS sample would be the ideal choice of bioinspired switchable surfaces.

Other than the two factors aforementioned, the contact time and preloading did not show strong influences on the adhesion force. All PDA–PDMS samples did not show a significant drop when the contact time and preloading were reduced. The adhesion forces of 0–5% PDA–PDMS samples decreased their adhesion forces by 7.1%, 6.6%, 23.2%, 19.5%, and 9.6%, with respect to changes in contact time (0–5 s). The preload force showed negligible impacts on the adhesion forces, as shown in Figure S3 in the Supporting Information. In contrast, the retraction velocity had a strong effect on the adhesion force. The maximum and minimum deviations of the adhesion force among 5% PDA–PDMS samples were 9721 nN and 4765 nN, respectively.

The PDA-PDMS biometric surfaces show a photothermal property, which can be improved with the doping percentage of TDPDA (see Figure S4 in the Supporting Information). Under 3 min of continuous NIR irradiation, the temperatures of 0–5% PDA-PDMS samples increased by 50.4%, 88.4%, 120%, 167.6%, and 221.2% respectively (Figure 2d). The photothermal properties of the PDA-PDMS surfaces were durable and reliable. For instance, the 5% PDA-PDMS surface was heated by NIR and cooled 30 times. Its photothermal effect minimally changed during and after the cyclic treatments (Figure 2e).

It is evident that the NIR irradiation could improve the detaching property of the TDPDA surfaces. When compared with the surfaces without treatment of the NIR irradiation, the treated surface had a stronger attenuation tendency in adhesion force under different retraction velocities. For example, the 5% TDPDA treated surface decreased by 48.44% when the retraction velocity decreased from 100 μ m/s to 10 μ m/s (Figure 2f). The retraction velocity is the velocity at which the AFM probe leaves the surface of the object after contact in the test. The variation of the adhesive forces and the effect of retraction velocities on other bioinspired surfaces prepared with or without NIR irradiation are shown in Figure S5 in the Supporting Information.

Self-Cleaning Capability of the Bioinspired Surface. This section is mainly focused on self-cleaning tests of the bioinspired surfaces under the following experimental conditions: (i) without NIR at 30 °C, (ii) without NIR at 50 °C, and (iii) with NIR at 30 °C. A load–drag–pull (LDP) procedure was applied to test the self-cleaning capability in air, as shown in Figures 3a and Figure 3b. The surface of the

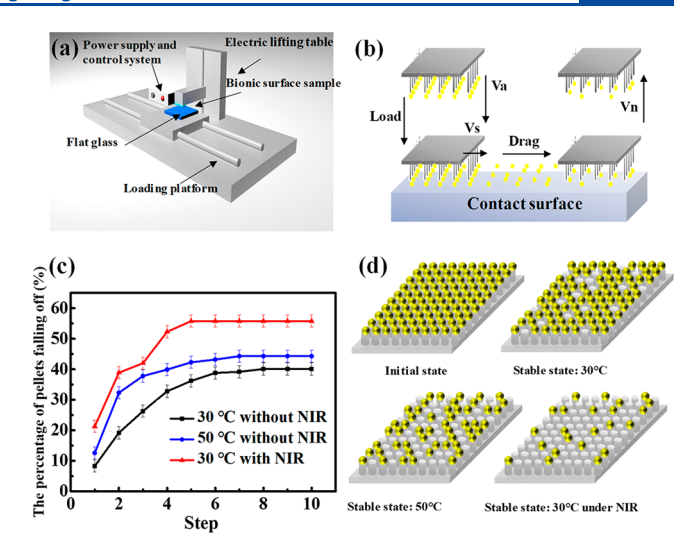


Figure 3. (a) Schematic of the self-cleaning testing apparatus. The preload of the self-cleaning experiments was kept as 2 N, and the velocity of the self-cleaning experiments was kept as 1 cm/s. (b) Schematic of the "load—drag—pull" (LDP) procedure. (c) Dislodging rate versus steps for the three conditions. (d) Self-cleaning mechanisms of bioinspired surface under different conditions.

opposing substrate was covered with glass slides adhered on a metal frame using a conductive adhesive (Lot No. FS05006). We chose the 5% PDA—PDMS surface in this section, since it demonstrated the most optimized behaviors in the previous experiments. The dislodging rate of polystyrene pellets (PS) microspheres after each step was recorded as a measure of the self-cleaning rate. The dislodging rate here is the ratio of the PS that have been transferred off the bioinspired surface to the PS that was on the initial bioinspired surface.

Under 30 °C, the sample with NIR treatment requested only 5 steps to reach a 55.8% in the PS-dislodging ratio (Figure 3c). In contrast, the sample without NIR treatment under the same temperature reached a only 40.1% dislodging ratio by 8 steps. In addition, the bioinspired surface without NIR treatment took 7 steps to obtain 44.3% of the dislodging ratio under 50 °C. The pure PDMS bioinspired surface required around 8 steps to achieve a 24.7% dislodging ratio (Figure S7 in the Supporting Information). It is evident that the self-cleaning effect of the bioinspired surfaces was enhanced as the temperature rose. (See Figure 3d, as well as Figure S6 in the Supporting Information.) In addition, the bioinspired surfaces doped with TDPDA were responsive to NIR, which reinforced the self-cleaning effect, even under the low temperature. Therefore, the addition of the TDPDA solution and the NIR treatment improved the self-cleaning capability of the bioinspired surface of the PDMS system.

The bioinspired surface was tested by the AFM probe with PS microparticles (\sim 10 nm) attached. The surfaces' adhesion decreased as the temperature increased. In the same situation, during the self-cleaning experiment, the PS microparticles (\sim 8 nm) dislodging rate also increased. The self-cleaning capability increased as the bioinspired surface temperature increased under NIR irradiation. The two contact scenarios between PS and bioinspired surfaces are shown in Figure S9 in the Supporting Information. To clarify the change of the adhesion force between the PS and the bioinspired surface, the Fourier-transform infrared spectroscopy (FTIR) spectra with different temperatures (30–50 $^{\circ}$ C) were performed (shown in Figure

4a). When the temperature increased from 30 °C to 50 °C, the C-N bond peak at 788.78 cm⁻¹ shifted to higher wave-

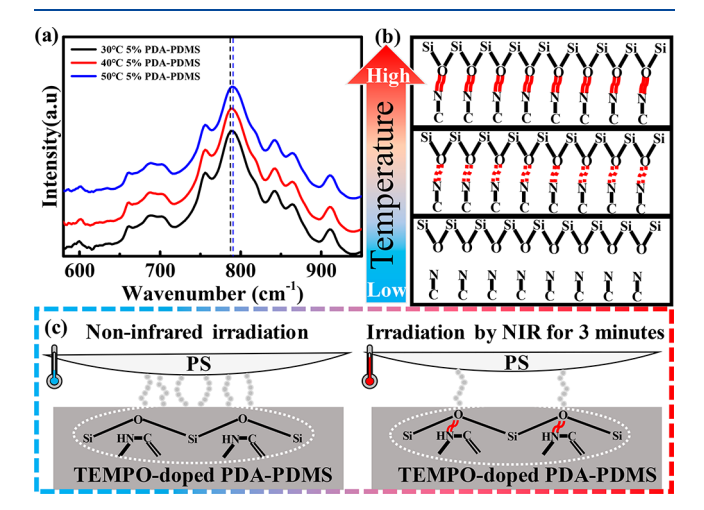


Figure 4. (a) Fourier transform infrared spectrometry (FTIR) spectra of the 5% PDA-PDMS sample at temperatures of 30, 40, and 50 °C. (b) Schematic of reduction of adhesion force with NIR irradiation. (c) Schematic diagram explaining the mechanism of adhesion reduction.

numbers without forming new peaks, which indicates no new bond formation. Hence, the peak shift was attributed to the reduction reaction. No wave peak appeared and moved at wavenumbers of 3200-3700 cm⁻¹ in FTIR, here we rule out the effect of hydrogen bonding (Figure S8 in the Supporting Information). The force between PS and the bioinspired surface is mainly caused by the van der Waals force.³⁰ However, with the NIR irradiation, TDPDA particles could significantly enhance the temperature of the bioinspired surface, because they had strong endothermic abilities.³³ It is expected that, because of the reduction of the C-N bond, the existence of the donor-acceptor molecular pair structure will be stronger and the unshared pair electrons will be reduced (in Figure 4b). Therefore, the intermolecular force between PS and the bioinspired surfaces will be reduced. This effect resulted in a decrease in the adhesion force during the attachment and detachment process. Thus, improvement of the self-cleaning capability was achieved (in Figure 4c).

CONCLUSION

In this study, we prepared a bioinspired photodetachable adhesive surface with high self-cleaning capability by using a PDMS-TEMPO-doped PDA hybrid materials system. Doping of TDPDA into the PDMS improved the adhesive properties of the bioinspired surfaces, and the adhesive force of the 5% TDPDA-PDMS surface decreased by 30%, compared with its initial adhesion force under 808-nm NIR irradiation. The addition of the TDPDA solution enabled the bioinspired surface to have strong photothermal effects. The temperature of the surfaces increased from room temperature to 80.3 °C under 3 min of NIR irradiation. At the same time, the bioinspired surfaces have a favorable characteristic for selfcleaning, in which the adhesion decreases as the temperature increases. It was evident that since the van der Waals between the PS and the bioinspired surface decreased, the bioinspired surfaces have a strong self-cleaning capability under the NIR irradiation. Under the optimized condition, only five steps are

required to achieve a self-cleaning rate of 55.8%. The innovation of realizing a feasible control of adhesion forces under noncontact external stimuli (e.g., NIR irradiation) opens a new door in designing higher performance and smart self-cleaning surfaces for many engineering, biomedical, and energy-related applications.

ASSOCIATED CONTENT

Solution Supporting Information

The Supporting Information is available free of charge at https://pubs.acs.org/doi/10.1021/acs.langmuir.1c00568.

SEM image of TEMPO-doped PDA (Figure S1). Contact angle tests of pure PDMS and 5% doping bioinspired surfaces to water at 30 °C, with various surfaces, and with/without microstructure (Figure S2). Dry adhesion performance of the bioinspired surfaces under various factors (Figure S3). Infrared thermal images of samples a-e under various NIR irradiation time periods (Figure S4). Effect of NIR on the adhesion of samples a-d under different retraction velocities (Figure S5). Photographs of bioinspired surfaces used in a ball drop test under various temperatures with NIR (Figure S6). . Dislodging rate versus steps for pure PDMS bioinspired surface, and a photograph of the PS microsphere on the pure PDMS bioinspired surface at the beginning and final states (Figure S7). Fourier transform infrared spectroscopy (FTIR) spectra of 5% PDA-PDMS samples at various wavenumbers (Figure S8). Schematic diagram of the contact state between the PS microparticle and bioinspired surfaces of an AFM adhesion test and a self-cleaning test (Figure S9) (PDF)

AUTHOR INFORMATION

Corresponding Authors

Quan Xu — State Key Laboratory of Heavy Oil Processing, China University of Petroleum (Beijing), Beijing 102249, China; occid.org/0000-0003-2195-2513;

Email: xuquan@cup.edu.cn

Hong Zhao — College of Mechanical Transportation Engineering, China University of Petroleum (Beijing), Beijing 102249, China; Email: hzhao_cn@163.com

Authors

Xiaohang Luo — State Key Laboratory of Heavy Oil Processing, China University of Petroleum (Beijing), Beijing 102249, China

Xiaoxiao Dong — College of Mechanical Transportation Engineering, China University of Petroleum (Beijing), Beijing 102249. China

Yanguang Hou — College of Mechanical Transportation Engineering, China University of Petroleum (Beijing), Beijing 102249, China

Lifu Zhang – State Key Laboratory of Heavy Oil Processing, China University of Petroleum (Beijing), Beijing 102249, China

Penghao Zhang — Energy, Environmental & Chemical Engineering, Washington University in St. Louis, St. Louis, Missouri 63130, United States

Jiaye Cai — State Key Laboratory of Heavy Oil Processing, China University of Petroleum (Beijing), Beijing 102249, China

- Ming Zhao State Key Laboratory of Heavy Oil Processing, China University of Petroleum (Beijing), Beijing 102249, China
- Melvin A. Ramos Department of Mechanical Engineering, California State University, Los Angeles, California 90032, United States
- Travis Shihao Hu Department of Mechanical Engineering, California State University, Los Angeles, California 90032, United States

Complete contact information is available at: https://pubs.acs.org/10.1021/acs.langmuir.1c00568

Author Contributions

^VThese authors contributed equally to this work.

Notes

The authors declare no competing financial interest.

ACKNOWLEDGMENTS

We gratefully acknowledge the financial support from National Nature Science Foundation of China (51875577), the Science Foundation of China University of Petroleum-Beijing (No. 2462020XKJS01), and the U.S. National Science Foundation (Award No. 2004251).

REFERENCES

- (1) Zhang, C.; McAdams, D. A., II.; Grunlan, J. C. Nano/Micro-Manufacturing of Bioinspired Materials: a Review of Methods to Mimic Natural Structures. *Adv. Mater.* **2016**, 28 (30), 6292–6321.
- (2) Drier, E. A.; Govind, S.; Steward, R. Cactus-independent regulation of Dorsal nuclear import by the ventral signal. *Curr. Biol.* **2000**, *10* (1), 23–26.
- (3) Zhang, C.; Zhang, B.; Ma, H.; Li, Z.; Xiao, X.; Zhang, Y.; Cui, X.; Yu, C.; Cao, M.; Jiang, L. Bioinspired Pressure-Tolerant Asymmetric Slippery Surface for Continuous Self-Transport of Gas Bubbles in Aqueous Environment. *ACS Nano* **2018**, *12* (2), 2048–2055.
- (4) Lin, A. G.; Ding, X. F.; Xie, Z. D.; Sun, B. Y. Mechanical Properties of the Natural Heterogeneous Composites. *Mater. Sci. Forum* **2009**, 628–629, 657–662.
- (5) Jiao, D.; Liu, Z.; Zhang, Z.; Zhang, Z. Intrinsic hierarchical structural imperfections in a natural ceramic of bivalve shell with distinctly graded properties. *Sci. Rep.* **2015**, 5 (1), 12418.
- (6) Zhang, C.; Gong, L.; Xiang, L.; Du, Y.; Hu, W.; Zeng, H.; Xu, Z.-K. Deposition and Adhesion of Polydopamine on the Surfaces of Varying Wettability. ACS Appl. Mater. Interfaces 2017, 9 (36), 30943—30950.
- (7) Autumn, K.; Liang, Y. A.; Hsieh, S. T.; Zesch, W.; Chan, W. P.; Kenny, T. W.; Fearing, R.; Full, R. J. Adhesive force of a single gecko foot-hair. *Nature* **2000**, 405 (6787), 681–685.
- (8) Autumn, K.; Sitti, M.; Liang, Y. A.; Peattie, A. M.; Hansen, W. R.; Sponberg, S.; Kenny, T. W.; Fearing, R.; Israelachvili, J. N.; Full, R. J. Evidence for van der Waals adhesion in gecko setae. *Proc. Natl. Acad. Sci. U. S. A.* **2002**, *99* (19), 12252.
- (9) Cadirov, N.; Booth, J. A.; Turner, K. L.; Israelachvili, J. N. Influence of Humidity on Grip and Release Adhesion Mechanisms for Gecko-Inspired Microfibrillar Surfaces. *ACS Appl. Mater. Interfaces* **2017**, 9 (16), 14497–14505.
- (10) Jeong, H. E.; Lee, J.-K.; Kim, H. N.; Moon, S. H.; Suh, K. Y. A nontransferring dry adhesive with hierarchical polymer nanohairs. *Proc. Natl. Acad. Sci. U. S. A.* **2009**, *106* (14), 5639.
- (11) Wang, J.; Le-The, H.; Wang, Z.; Li, H.; Jin, M.; van den Berg, A.; Zhou, G.; Segerink, L. I.; Shui, L.; Eijkel, J. C. T. Microfluidics Assisted Fabrication of Three-Tier Hierarchical Microparticles for Constructing Bioinspired Surfaces. *ACS Nano* **2019**, *13* (3), 3638–3648
- (12) Wang, Z. Slanted Functional Gradient Micropillars for Optimal Bioinspired Dry Adhesion. ACS Nano 2018, 12 (2), 1273–1284.

- (13) Xue, L.; Xie, W.; Driessen, L.; Domke, K. F.; Wang, Y.; Schlücker, S.; Gorb, S. N.; Steinhart, M. Advanced SERS Sensor Based on Capillarity-Assisted Preconcentration through Gold Nanoparticle-Decorated Porous Nanorods. *Small* **2017**, *13* (22), 1603947.
- (14) Guo, T.; Heng, L.; Wang, M.; Wang, J.; Jiang, L. Robust Underwater Oil-Repellent Material Inspired by Columnar Nacre. *Adv. Mater.* **2016**, 28 (38), 8505–8510.
- (15) Priemel, T.; Degtyar, E.; Dean, M. N.; Harrington, M. J. Rapid self-assembly of complex biomolecular architectures during mussel byssus biofabrication. *Nat. Commun.* **2017**, *8* (1), 14539.
- (16) Bartlett, M. D.; Crosby, A. J. High Capacity, Easy Release Adhesives From Renewable Materials. *Adv. Mater.* **2014**, *26* (21), 3405–3409.
- (17) Qu, L.; Dai, L. Gecko-Foot-Mimetic Aligned Single-Walled Carbon Nanotube Dry Adhesives with Unique Electrical and Thermal Properties. *Adv. Mater.* **2007**, *19* (22), 3844–3849.
- (18) Raut, H. K.; Baji, A.; Hariri, H. H.; Parveen, H.; Soh, G. S.; Low, H. Y.; Wood, K. L. Gecko-Inspired Dry Adhesive Based on Micro-Nanoscale Hierarchical Arrays for Application in Climbing Devices. ACS Appl. Mater. Interfaces 2018, 10 (1), 1288–1296.
- (19) Geim, A. K.; Dubonos, S. V.; Grigorieva, I. V.; Novoselov, K. S.; Zhukov, A. A.; Shapoval, S. Y. Microfabricated adhesive mimicking gecko foot-hair. *Nat. Mater.* **2003**, *2* (7), 461–463.
- (20) Murphy, M. P.; Kim, S.; Sitti, M. Enhanced Adhesion by Gecko-Inspired Hierarchical Fibrillar Adhesives. *ACS Appl. Mater. Interfaces* **2009**, *1* (4), 849–855.
- (21) Autumn, K.; Majidi, C.; Groff, R. E.; Dittmore, A.; Fearing, R. Effective elastic modulus of isolated gecko setal arrays. *J. Exp. Biol.* **2006**, 209 (18), 3558.
- (22) Kustandi, T. S.; Samper, V. D.; Yi, D. K.; Ng, W. S.; Neuzil, P.; Sun, W. Self-Assembled Nanoparticles Based Fabrication of Gecko Foot-Hair-Inspired Polymer Nanofibers. *Adv. Funct. Mater.* **2007**, *17* (13), 2211–2218.
- (23) Liu, K.; Du, J.; Wu, J.; Jiang, L. Superhydrophobic gecko feet with high adhesive forces towards water and their bio-inspired materials. *Nanoscale* **2012**, *4* (3), 768–772.
- (24) Yu, J.; Chary, S.; Das, S.; Tamelier, J.; Pesika, N. S.; Turner, K. L.; Israelachvili, J. N. Gecko-Inspired Dry Adhesive for Robotic Applications. *Adv. Funct. Mater.* **2011**, *21* (16), 3010–3018.
- (25) Qu, L.; Dai, L.; Stone, M.; Xia, Z.; Wang, Z. L. Carbon nanotube arrays with strong shear binding-on and easy normal lifting-off. *Science* **2008**, 322 (5899), 238–242.
- (26) Xu, M.; Du, F.; Ganguli, S.; Roy, A.; Dai, L. Carbon nanotube dry adhesives with temperature-enhanced adhesion over a large temperature range. *Nat. Commun.* **2016**, 7 (1), 13450.
- (27) Murphy, M. P.; Aksak, B.; Sitti, M. Gecko-Inspired Directional and Controllable Adhesion. *Small* **2009**, *5* (2), 170–175.
- (28) Li, M.; Xu, Q.; Wu, X.; Li, W.; Lan, W.; Heng, L.; Street, J.; Xia, Z. Tough Reversible Adhesion Properties of a Dry Self-Cleaning Biomimetic Surface. *ACS Appl. Mater. Interfaces* **2018**, *10* (31), 26787–26794.
- (29) Chen, P.; Li, X.; Ma, J.; Zhang, R.; Qin, F.; Wang, J.; Hu, T. S.; Zhang, Y.; Xu, Q. Bioinspired Photodetachable Dry Self-Cleaning Surface. *Langmuir* **2019**, 35 (19), 6379–6386.
- (30) Xu, Q.; Wan, Y.; Hu, T. S.; Liu, T. X.; Tao, D.; Niewiarowski, P. H.; Tian, Y.; Liu, Y.; Dai, L.; Yang, Y.; Xia, Z. Robust self-cleaning and micromanipulation capabilities of gecko spatulae and their biomimics. *Nat. Commun.* **2015**, *6* (1), 8949.
- (31) Saitaer, X.; Sanbhal, N.; Qiao, Y.; Li, Y.; Gao, J.; Brochu, G.; Guidoin, R.; Khatri, A.; Wang, L. J. C. Polydopamine-Inspired Surface Modification of Polypropylene Hernia Mesh Devices via Cold Oxygen Plasma: Antibacterial and Drug Release Properties. *Coatings* **2019**, 9 (3), 164.
- (32) Wan, P.; Zhao, N.; Qi, F.; Zhang, B.; Xiong, H.; Yuan, H.; Liao, B.; Ouyang, X. Synthesis of PDA-BN@f-Al₂O₃ hybrid for nanocomposite epoxy coating with superior corrosion protective properties. *Prog. Org. Coat.* **2020**, *146*, 105713.
- (33) Usta, D. D.; Celebi, N.; Soysal, F.; Saglam, A. S. Y.; Yildiz, N.; Salimi, K. Bio-inspired NIR responsive Au-pDA@pDA sandwich

- nanostructures with excellent photo-thermal performance and stability. *Colloids Surf., A* **2021**, *611*, 125758.
- (34) Mei, S.; Xu, X.; Priestley, R. D.; Lu, Y. Polydopamine-based nanoreactors: synthesis and applications in bioscience and energy materials. *Chem. Sci.* **2020**, *11*, 12269.
- (35) Chen, Y.; Zhang, F.; Wang, Q.; Lin, H.; Tong, R.; An, N.; Qu, F. The synthesis of LA-Fe $_3$ O $_4$ @PDA-PEG-DOX for photothermal therapy—chemotherapy. *Dalton Trans.* **2018**, 47, 2435.
- (36) Zou, Y.; Chen, X.; Yang, P.; Liang, G.; Yang, Y.; Gu, Z.; Li, Y. Regulating the absorption spectrum of polydopamine. *Sci. Adv.* **2020**, 6 (36), eabb4696.
- (37) Xu, Q.; Li, M.; Niu, J.; Xia, Z. Dynamic Enhancement in Adhesion Forces of Microparticles on Substrates. *Langmuir* **2013**, 29 (45), 13743–13749.
- (38) Xu, Q.; Li, M.; Zhang, L.; Niu, J.; Xia, Z. Dynamic Adhesion Forces between Microparticles and Substrates in Water. *Langmuir* **2014**, 30 (37), 11103–11109.